Thermochimica Acta, 144 (1989) 83–93
Elsevier Science Publishers B.V., Amsterdam – Printed in The Netherlands

THERMAL DEHYDRATION OF CRYSTALLINE $NiSO_4 \cdot 6H_2O$

S.G. SINHA and N.D. DESHPANDE

Physics Department, Institute of Science, Nagpur 440 001 (India)

D.A. DESHPANDE

Physics Department, V.M.V. Commerce, J.M.T. Arts and J.J.P. Science College, Wardhaman Nagar, Nagpur 440 008 (India)

(Received 20 July 1988)

ABSTRACT

The thermal dehydration of hexahydrated nickel sulphate crystals grown by slow evaporation of aqueous solution maintained at $40 \pm 1°C$ have been studied using dynamic and isothermal TG techniques. The dynamic TG measurements suggest the scheme of dehydration to be 1 mol, 2 mol, 2 mol and 1 mol at mean temperatures of 143, 180, 230 and 358 °C, respectively. However, isothermal measurements suggest that the dehydration scheme is temperature-dependent. Many features of random nucleation and growth have been observed on the (001) face of the crystal under an optical microscope. The isothermal and dynamic TG measurements together with the optical microscopic study suggest that the dehydration of $NiSO_4 \cdot 6H_2O$ proceeds through random nucleation and growth. The proper form of $F(\alpha)$ could not be decided.

INTRODUCTION

The thermal dehydration of $NiSO_4 \cdot 6H_2O$ and $NiSO_4 \cdot 7H_2O$ has been discussed by several workers. Ben Dor and Margalith [1] have studied many polyhydrated metal sulphates and report that all but one of the water molecules are evolved at relatively low temperatures (beginning at 60 °C), and then after a significant rise in temperature the last molecule is evolved. Tanabe and co-workers [2] have used X-ray, IR, ESR and NMR techniques in their investigations of $NiSO_4 \cdot H_2O$ because of their special interest in the catalytic activity. Fruchart and Michel [3] give the dehydration steps of $NiSO_4 \cdot 7H_2O$ as 1 mol, 2 mol, 3 mol and 1 mol. From simultaneous TG, DTG and DTA analyses of $NiSO_4 \cdot 7H_2O$, Sarig [4] suggests that the dehydration steps are 1 mol, 3 mol, 2 mol and 1 mol taking place at temperatures of 60, 110, 130 and 330 °C, respectively. Kher and co-workers [5] in their study of the dehydration of hexa- and heptahydrates of $NiSO_4$ gave the sequence of dehydration for $NiSO_4 \cdot 7H_2O$ crystals as 1 mol, 3 mol,

0040-6031/89/$03.50

2 mol and 1 mol at temperatures of 130, 190, 210 and 380 °C, and the sequence for $NiSO_4 \cdot 6H_2O$ crystals as 1 mol, 2 mol, 2 mol and 1 mol at temperatures of 129, 187, 214 and 390 °C. These workers have also observed that crystals and packed powders behave differently as regards thermal dehydration. Rabbering et al. [6] have reviewed these contradictory reports concerning the dehydration of hexa- and heptahydrates of $NiSO_4$ and, using DSC, DTA, TG and X-ray methods, have attempted to clarify the dehydration pathway. Friesen et al. [7] have used X-ray and DSC techniques to study dehydration and phase transition in hexa- and heptahydrates of nickel sulphates. They have observed that $NiSO_4 \cdot 7H_2O$ dehydrates spontaneously via $7 \rightarrow 6\beta \rightarrow 6\alpha$ at room temperature, while the dehydration pathway of $NiSO_4 \cdot 6H_2O$ is $6\alpha \rightarrow 6\gamma \rightarrow 4 \rightarrow 1$.

A survey of the literature has indicated that although some work on the optical microscopy and kinetics of the dehydration of $NiSO_4 \cdot 7H_2O$ [8] and $NiSO_4 \cdot 6H_2O$ [9] has been carried out, no studies of the kinetics of the various dehydration steps, nor of the products formed during dehydration have been published. This paper reports on an attempt to study the mechanism of dehydration of $NiSO_4 \cdot 6H_2O$ using isothermal TG, dynamic TG and optical microscopic techniques.

EXPERIMENTAL

AnalaR Grade nickel sulphate was obtained from Merck. Hexahydrated crystals of nickel sulphate were grown by slow evaporation of the aqueous solution. The temperature of the solution was maintained at 40 ± 1 °C.

A TG study was carried out using a TG assembly fabricated in the laboratory, details of which are given elsewhere [10]. Measurement of mass loss was carried out in the temperature range 30–500 °C. The crystals were heated at a rate of 5 °C min^{-1}. The value of $\Delta m/\Delta t$, i.e. rate of change of mass (mg min^{-1}) was calculated for different temperatures. Curves of change in mass vs. temperature (TG) and rate of change of mass vs. temperature (differential thermogravimetry, DTG) were plotted.

Isothermal TG measurements were carried out by maintaining the temperature constant within ±1 °C. Measurements of loss in mass were made in two temperature ranges: (i) 180, 190, 200 and 210 °C; and (ii) 310, 320, 330 and 340 °C.

An optical microscopic study was carried out on the crystals using a reflecting microscope. A freshly prepared crystal was taken out of a supersaturated solution and dried. First the original crystal surface was studied for nucleations. It was then heated for 1–2 min on a hot plate maintained at 80 °C and the same crystal surface was observed again under the microscope. This procedure was repeated a number of times. Heating time was decided by visual inspection of the crystal.

RESULTS AND DISCUSSION

Figure 1 shows representative curves (TG and DTG) for the sequence of dehydration steps for the $NiSO_4 \cdot 6H_2O$ crystal grown at 40 °C. It can be seen that there are four DTG maxima at mean temperatures of 143, 190, 230 and 358 °C. There also occur changes of slope in the temperature ranges (100–140, 140–180, 180–210 and 330–380 °C), indicating four dehydration steps. For a crystal of mass 150 mg the observed loss in mass corresponded to six water molecules.

The TG measurements (dynamic) suggest the following scheme of dehydration with respect to temperature.

$$NiSO_4 \cdot 6H_2O \xrightarrow{143\,^\circ C} NiSO_4 \cdot 5H_2O + H_2O$$

$$NiSO_4 \cdot 5H_2O \xrightarrow{180\,^\circ C} NiSO_4 \cdot 3H_2O + 2H_2O$$

$$NiSO_4 \cdot 3H_2O \xrightarrow{230\,^\circ C} NiSO_4 \cdot H_2O + 2H_2O$$

$$NiSO_4 \cdot H_2O \xrightarrow{358\,^\circ C} NiSO_4 + H_2O$$

This scheme of dehydration is similar to that reported by Kher et al. [5] for $NiSO_4 \cdot 6H_2O$.

From the mass loss measurements, the fraction α dehydrated at a particular temperature T was calculated. Figure 2 is a plot of α vs. T. This curve shows four different regions, corresponding to loss of 1, 2, 2 and 1 molecules

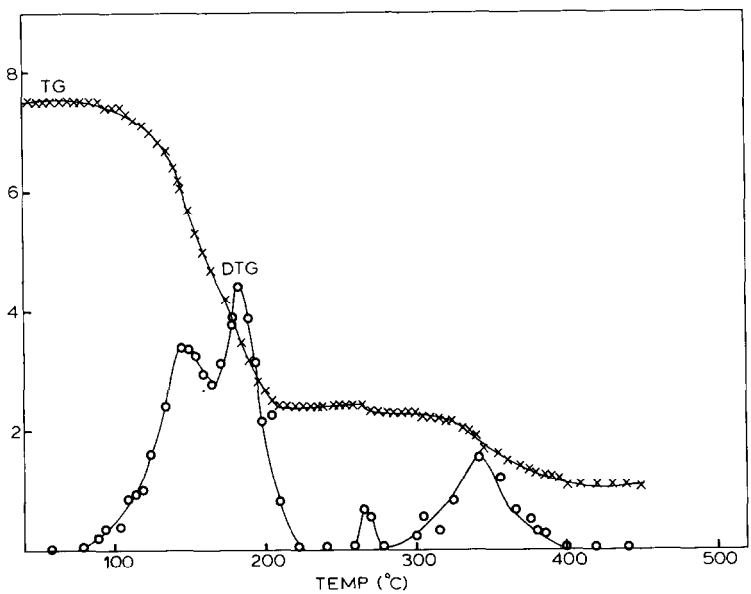

Fig. 1. TG and DTG curves for the thermal analysis of crystalline $NiSO_4 \cdot 6H_2O$.

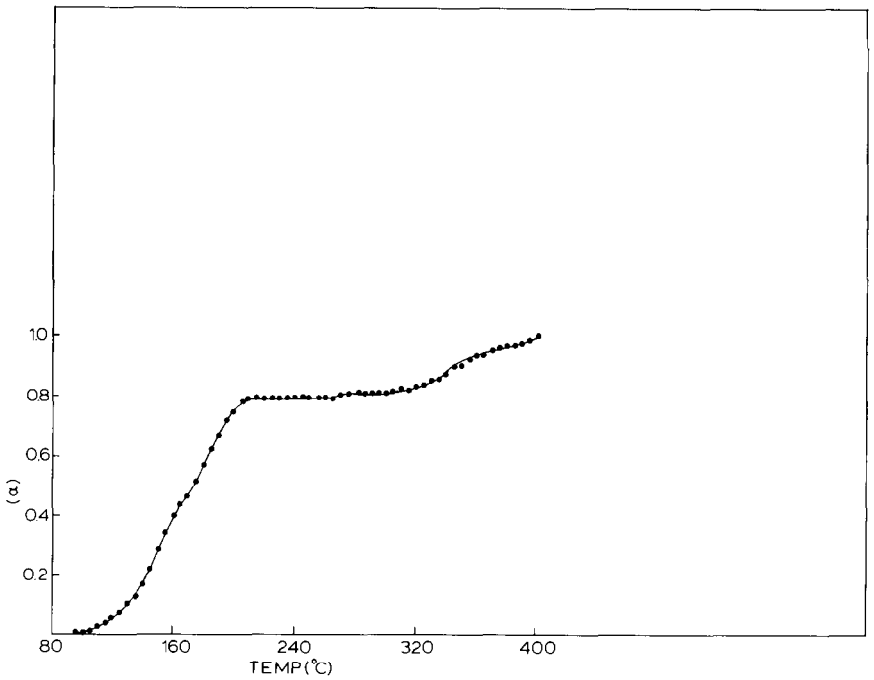

Fig. 2. Plot of α vs. T for crystalline $NiSO_4 \cdot 6H_2O$.

of water, respectively, which confirms the dehydration steps given by the DTG analysis. Values for E and Z were calculated from dynamic TG measurements, making use of the Coats and Redfern equation [11]

$$\ln\left\{\frac{F(\alpha)}{T^2}\right\} = \ln\left\{\frac{ZR}{\phi E}\left(1 - \frac{2RT}{E}\right)\right\} - \frac{E}{RT} \tag{1}$$

where T is the absolute temperature, Z is the frequency factor, R is the gas constant, ϕ is the linear heating rate, and E is the activation energy. Figure 3 shows a typical plot of $-\log\{F(\alpha)/T^2\}$ vs. $1/T$, where $F(\alpha) = -\log(1-\alpha)^n$ and $n = 1$, 0.66, 0.5, 0.4, 0.33 and 0.25. It can be seen that all the functions give straight-line plots, and there are four slope changes in a curve, indicative of four dehydration steps. There is also a straight line plot with an opposite slope, in the temperature range in between the two dehydration regions (after the removal of five water molecules and prior to the removal of the sixth). However this plot is of no significance because there is no loss in crystal mass with the change in temperature within this range. Kinetic parameters obtained for the dehydration of $NiSO_4 \cdot 6H_2O$ using different forms of $F(\alpha)$ are given in Table 1.

Isothermal TG measurements were carried out in two different temperature ranges, 180–210 and 310–340 °C, at intervals of 10 °C. Figure 4 shows the plot of the fraction α dehydrated at time t, against time at temperatures

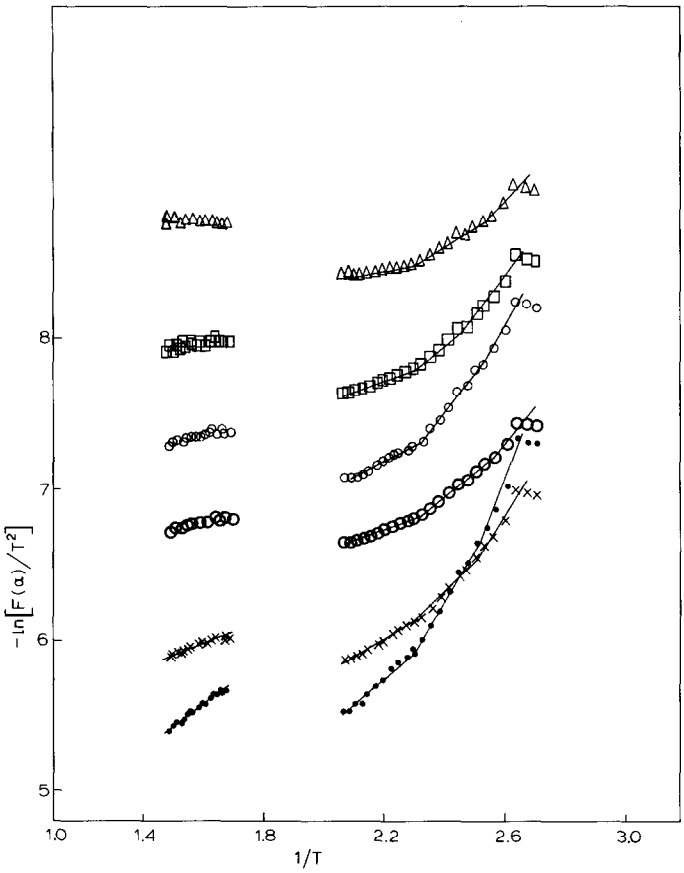

Fig. 3. Plots of $-\ln(F(\alpha)/T^2)$ vs. $1/T$ for the thermal dehydration of crystalline $NiSO_4 \cdot 6H_2O$ (dynamic): •, $n=1$; ×, $n=0.66$; ○, $n=0.5$; ○, $n=0.4$; □, $n=0.33$; △, $n=0.25$. The scale marked along the y-axis is for $n=1$. For other functions the scale was altered as appropriate for drawing the remaining curves.

180, 190, 200 and 210 °C. The mass loss measurements in this temperature range correspond to five water molecules out of the total six in the crystal. It can be seen that the lower the isothermal temperature, the longer the time required for the release of the five water molecules. Similar results are obtained in the temperature range 310–340 °C. For the calculation of kinetic parameters from isothermal measurements, it was assumed that the equation

$$d\alpha/dt = kf(\alpha) \tag{2}$$

holds good for the isothermal dehydration of $NiSO_4 \cdot 6H_2O$, where α is the fraction dehydrated at time t, and k is the rate constant. Integration of eqn. (2) gives

$$F(\alpha) = \int (d\alpha/f(\alpha)) = tZ \exp(-E/RT) \tag{3}$$

TABLE 1

Functions $F(\alpha)$ and kinetic parameters for the thermal dehydration of $NiSO_4 \cdot 6H_2O$ from dynamic TG

$F(\alpha)$	E (kcal mol^{-1})			
	Step 1	Step 2	Step 3	Step 4
$-\log(1-\alpha)$	26.40 ± 2.73	16.53 ± 1.72	8.65 ± 0.60	6.67 ± 1.01
$(-\log(1-\alpha))^{0.66}$	17.29 ± 2.73	9.71 ± 0.81	5.16 ± 0.20	3.18 ± 0.46
$(-\log(1-\alpha))^{0.5}$	12.29 ± 2.12	8.49 ± 2.22	4.10 ± 0.46	2.73 ± 0.5
$(-\log(1-\alpha))^{0.4}$	9.10 ± 1.82	5.76 ± 0.40	2.58 ± 0.20	
$(-\log(1-\alpha))^{0.33}$	8.64 ± 1.36	4.10 ± 0.46	1.82 ± 0.5	
$(-\log(1-\alpha))^{0.25}$	5.69 ± 1.14	3.33 ± 0.81		
$F(\alpha)$	Z (s^{-1})			
	Step 1	Step 2	Step 3	Step 4
$-\log(1-\alpha)$	$(5.47 \pm 3.07) \times 10^{25}$	$(1.61 \pm 0.80) \times 10^{18}$	$(1.00 \pm 0.35) \times 10^{13}$	$(5.5 \pm 1.7) \times 10^{11}$
$(-\log(1-\alpha))^{0.66}$	$(4.78 \pm 1.82) \times 10^{19}$	$(1.01 \pm 0.41) \times 10^{14}$	$(6.34 \pm 0.30) \times 10^{10}$	$(3.31 \pm 0.52) \times 10^{9}$
$(-\log(1-\alpha))^{0.5}$	$(1.70 \pm 0.63) \times 10^{16}$	$(1.13 \pm 0.34) \times 10^{13}$	$(1.30 \pm 0.16) \times 10^{10}$	$(4.63 \pm 0.66) \times 10^{9}$
$(-\log(1-\alpha))^{0.4}$	$(1.01 \pm 0.23) \times 10^{14}$	$(2.02 \pm 0.37) \times 10^{11}$	$(2.14 \pm 0.12) \times 10^{9}$	
$(-\log(1-\alpha))^{0.33}$	$(3.99 \pm 0.57) \times 10^{13}$	$(1.85 \pm 0.27) 10^{10}$	$(4.27 \pm 0.99) \times 10^{9}$	
$(-\log(1-\alpha))^{0.25}$	$(3.36 \pm 0.47) \times 10^{11}$	$(5.57 \pm 0.65) \times 10^{9}$		
	Dehydration temperature (°C)			
	Step 1	Step 2	Step 3	Step 4
	143 ± 2.2	180 ± 5	230 ± 12	358 ± 5.6

In order to obtain the function $F(\alpha)$ which describes the mechanism of isothermal dehydration, various theoretical functions are plotted against time t. The correct function should give a straight line with slope k, from which the mechanistic function [12] describing the reaction mechanism can be determined.

Typical plots of $F(\alpha)$ vs. time t in the temperature ranges 180–210 and 310–340 °C are shown in Fig. 5. (curves a and b respectively). It can be seen that the plot of $F(\alpha)$ vs. t is a straight line for some values of $F(\alpha)$. Figures 5a and b show two slope changes in the curve. These slope changes, together with the mass loss measurements, suggest the following dehydration scheme with respect to time for $NiSO_4 \cdot 6H_2O$.

$$NiSO_4 \cdot 6H_2O \xrightarrow{5\text{min}} NiSO_4 \cdot 4H_2O + 2H_2O \xrightarrow{16\text{min}} NiSO_4 \cdot H_2O + 3H_2O$$

$(T = 180\,°C)$

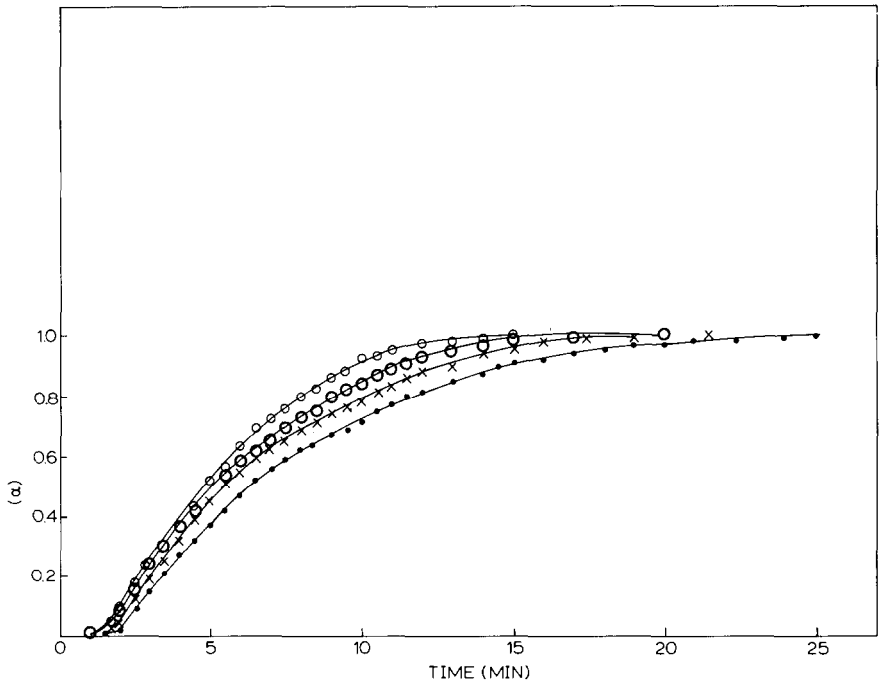

Fig. 4. Plots of fraction reacted α vs. time t: ·180 °C; ×, 190 °C; O, 200 °C; o, 210 °C.

$$NiSO_4 \cdot 6H_2O \xrightarrow{5min} NiSO_4 \cdot H_2O + 5H_2O \xrightarrow{25min} NiSO_4 + H_2O$$

$(T = 310\,°C)$

A typical plot of $-\log k$ versus $1/T$ for the two temperature ranges is shown in Fig. 6 (curves a and b respectively). Values for E and Z were calculated using the Arrhenius equation for the various dehydration steps, and are given in Table 2.

As reported in our earlier communications [13,14], a number of workers have suggested that correct dehydration mechanism, activation energy and frequency factor can be obtained by comparing information from both dynamic and static measurements. When the data presented in Tables 1 and 2 are compared, it is observed that there is no agreement in the values of E and Z for any step. This lack of agreement may be due to the following factors: (1) dehydration steps being different in dynamic and isothermal measurements; (2) the difference in the time available for dehydration in isothermal and dynamic studies; (3) the amount of water vapour pressure built up inside the crystal, owing to the difference in the time available for dehydration; and (4) a change in the number of paths available for dehydration.

Though no exact estimate of the values of E and Z can be made, our measurements suggest that the dehydration occurs through random nucleation and growth.

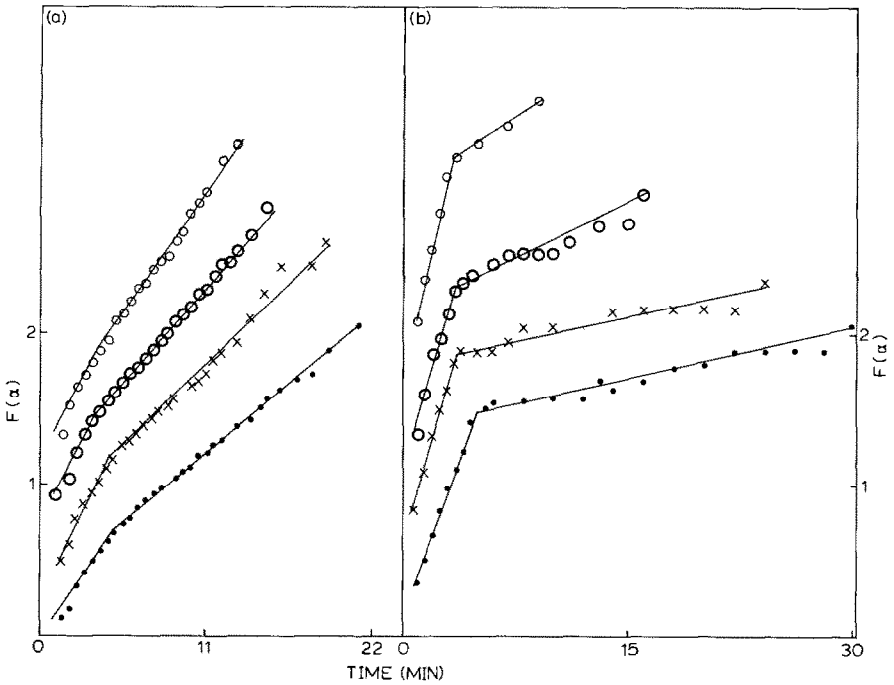

Fig. 5. Plots of $F(\alpha)$ (isothermal) vs. time t for a function $F(\alpha) = (-\log(1-\alpha))^{0.5}$ at (a) 180, 190, 200 and 210 °C and (b) 310, 320, 330 and 340 °C. •, 180 and 310 °C; ×, 190 and 320 °C; O, 200 and 330 °C; o, 210 and 340 °C. The scale marked along the y-axis is for •. For other temperatures the scale was altered as appropriate.

To verify the dehydration mechanism, a microscopic study of the crystal surface, successively heated at a constant temperature of 80 °C for 1–2 min, was carried out. Plates 1 to 5 show the results of the microscopic observation on the (001) face of the crystal.

Plate 1 shows the surface of the original hexahydrate crystal. It can be seen that there are some hollows as well as dark inclusion boundaries and dislocation sites which are randomly oriented. Note also the roughly hexagonal shape of the liquid inclusions (dark areas). Plate 2 shows a micrograph of the same crystal after heating for 1–2 minutes. A dehydration band (path), visible in the top right-hand corner, develops as the dehydration reaction proceeds. Plates 3, 4 and 5 show that this band (path) grows in dimension on successive heatings. A number of dehydration bands (paths) as well as patches are also seen to appear on successive heatings. The dehydration patches grow further in size (see Plate 4). This growth (bands and patches) with heating shows that dislocations are responsible for increased reactivity. The bands also provide evidence of preferential reaction at small angle boundaries like AB and CD. The microscopic study suggests that the dehydration on the (001) face in the initial stage is governed by inclusions and dislocations. Some of the dehydrating nuclei at the disloca-

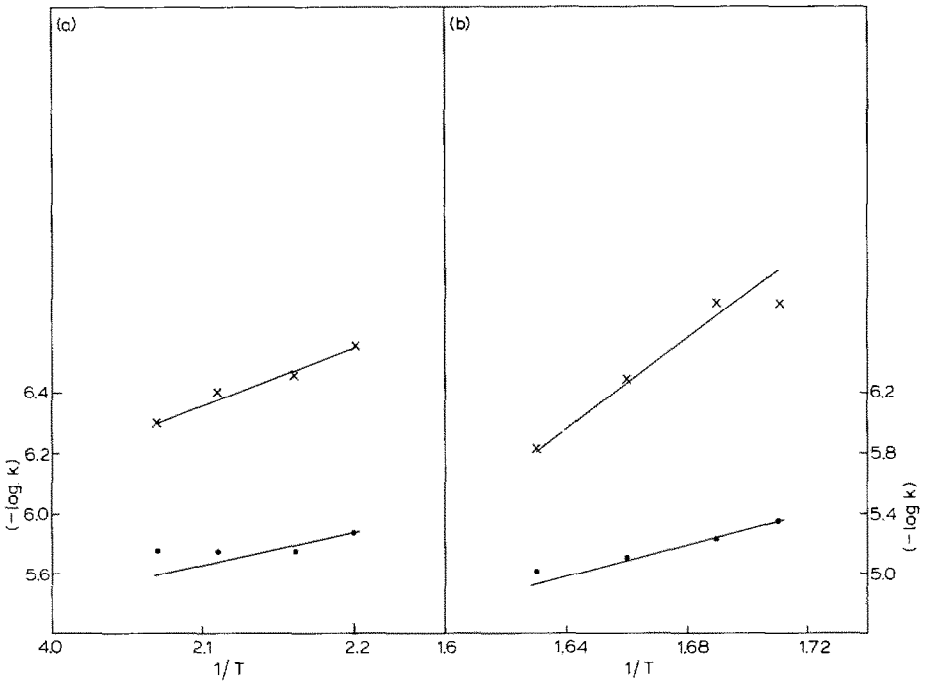

Fig. 6. Arrhenius plots for the isothermal dehydration of crystalline $NiSO_4 \cdot 6H_2O$ for $F(\alpha) = (-\log(1-\alpha))^{0.5}$ in the temperature ranges (a) 180–210 °C and (b) 310–340 °C, the two dehydration steps in each of the two temperature ranges consisting of 2 mol and 3 mol, and 5 mol and 1 mol, respectively. The scale marked along the ordinate is for the first step. The scale for the second step was altered. •, first step; ×, second step.

TABLE 2

Functions $F(\alpha)$ and kinetic parameters for the thermal dehydration of $NiSO_4 \cdot 6H_2O$ from isothermal TG

$F(\alpha)$	Step	Temperature range			
		180–210 °C		310–340 °C	
		E (kcal mol^{-1})	Z (s^{-1})	E (kcal mol^{-1})	Z (s^{-1})
$-\log(1-\alpha)$	1	–	–	17.78	$(3.77 \pm 0.35) \times 10^4$
	2	–	–	34.57	$(1.06 \pm 0.25) \times 10^{10}$
$(-\log(1-\alpha))^{0.66}$	1	5.43	1.18 ± 0.10	11.85	$(1.83 \pm 0.06) \times 10^2$
	2	6.42	2.79 ± 0.17	30.62	$(1.65 \pm 0.19) \times 10^8$
$(-\log(1-\alpha))^{0.5}$	1	6.42	3.42 ± 0.37	11.85	$(1.14 \pm 0.27) \times 10^2$
	2	8.39	16.88 ± 0.75	30.62	$(1.23 \pm 0.28) \times 10^8$
$(-\log(1-\alpha))^{0.4}$	1	6.91	5.70 ± 0.85	12.84	$(2.51 \pm 0.32) \times 10^2$
	2	6.91	2.67 ± 0.08	19.76	$(9.46 \pm 1.34) \times 10^3$
$(-\log(1-\alpha))^{0.33}$	1	4.94	0.68 ± 0.09	10.86	40.96 ± 3.00
	2	6.42	1.40 ± 0.06	35.57	$(5.42 \pm 1.56) \times 10^9$
$(-\log(1-\alpha))^{0.25}$	1	6.91	5.54 ± 1.17	11.85	74.38 ± 4.36
	2	8.39	8.13 ± 0.31	34.58	$(1.70 \pm 0.50) \times 10^9$

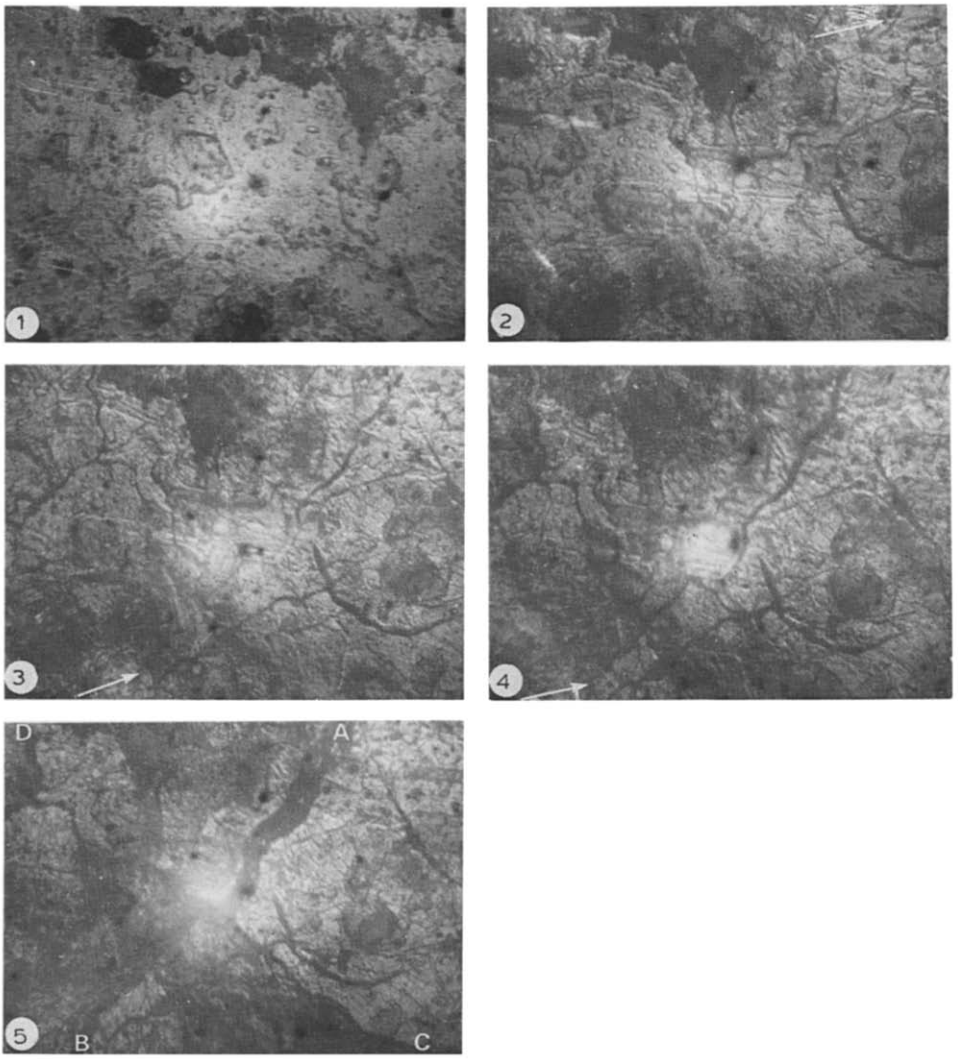

Plate 1. A region of the (001) face of the original nickel sulphate hexahydrate crystal. Hollows and dark inclusion boundaries and dislocations can be observed. Note also the roughly hexagonal shape of the liquid inclusions (dark area). (×400)

Plate 2. Micrograph of the same region as in Plate 1, after heating. A dehydration band can be seen in the top right-hand corner (see arrow). (×400)

Plates 3 and 4. The dehydration bands grow in size and in number, as do the dehydration patches (see arrow). (×400)

Plate 5. Dehydration bands such as AB and CD indicate preferential reaction at small angle boundaries. (×400)

tion sites grow in the form of a band, giving rise to dislocation multiplication on the (001) face. Though this is observed on the (001) face, it is likely that the same phenomenon occurs on the other faces too.

Thus dynamic and isothermal TG measurements in association with an optical microscopic study suggest that the mechanism of dehydration is one of random nucleation and growth. The same mechanism is described by different functions in isothermal and dynamic measurements.

CONCLUSION

The dynamic TG study gave the dehydration scheme as 1 mol, 2 mol, 2 mol and 1 mol, at temperatures of 143, 180, 230 and 358 °C respectively, whereas the isothermal TG study gave a different dehydration scheme dependent on temperature. Though no exact estimates of the values of E and Z for the dehydration process could be made, it can be said that the phenomenon proceeds through random nucleation and growth.

REFERENCES

1 L. Ben Dor and R. Margalith, Inorg. Chim. Acta, 1 (1967) 49.
2 T. Takeshita, R. Ohnishi, T. Matsui and K. Tanabe, J. Phys. Chem. 69 (1965) 4077.
3 R. Fruchart and A. Michel, C.R. Acad. Sci., 246 (1958) 1222.
4 S. Sarig, Thermochim. Acta, 7 (1973) 297.
5 P.N. Nandi, D.A. Deshpande and V.G. Kher, Thermochim. Acta, 32 (1979) 143.
6 G. Rabbering, J. Waurooy and A. Schniff, Thermochim. Acta, 12 (1975) 57.
7 M. Friesen, H.M. Burt and A.G. Mitchell, Thermochim. Acta, 41 (1980) 167.
8 W.E. Garner and W.R. Southon, J. Chem. Soc., (1935) 1705.
9 J.M. Thomas and G.D. Renshaw, J. Chem. Soc., A (1969) 2749; 2753; 2756.
10 P.N. Nandi, D.A. Deshpande and V.G. Kher, Proc. Indian Acad. Sci., Sect. A, 88 (1979) 130.
11 A.W. Coats and J.P. Redfern, Nature, 201 (1964) 68.
12 H. Tanaka, Thermochim. Acta, 46 (1981) 139.
13 S.G. Sinha, N.D. Deshpande and D.A. Deshpande, Thermochim. Acta, 113 (1987) 95.
14 S.G. Sinha, N.D. Deshpande and D.A. Deshpande, Thermochim. Acta., in press.